LIDAR Extended Object Tracking of a Maritime Vessel Using an Ellipsoidal Contour Model

Kristian Amundsen Ruud
Department of Mathematical Sciences
NTNU
Trondheim, Norway

Edmund Førland Brekke
Department of Engineering Cybernetics
NTNU
Trondheim, Norway

Jo Eidsvik
Department of Mathematical Sciences
NTNU
Trondheim, Norway

***Abstract*—Extended object tracking (EOT) plays an important role when creating autonomous systems like self-driving cars or surface vehicles. For accurate estimation of the target extent, it is important to have a sensor with high resolution and low measurement noise. In this paper we use the LIDAR sensor to track a single elliptical target in clutter with a contour measurement model. The model enables the use of extended Kalman filter (EKF) which is combined with a generalized probabilistic data association (GPDA) filter. The EKF method comes favorably out of a comparison with a random matrix parametrized EOT approach. The testing is done through simulation studies and on real LIDAR data from a passenger boat.**

I. Introduction

Autonomous systems emerge rapidly in several industries. In the maritime industry there is a growing interest in developing autonomous surface vehicles (ASVs) to do various tasks that are time consuming for human operators. When designing such vehicles it is important to give the system an accurate representation of the surroundings by using different sensors like radar, LIDAR, camera and infrared light.

In traditional target tracking the point target assumption is made, which means that at most one measurement comes from the target at each time step. When using sensors with high resolution this assumption is likely not valid, and the concept of extended object tracking (EOT) is relevant. When receiving several measurements from a target it is possible to calculate the extent shape in addition to the kinematic properties.

An approach for tracking elliptically shaped objects by using random matrices was first presented in [1] as a method for tracking a single extended target or a group of point targets from radar data. It was later modified in [2] by introducing sensor noise in the measurement modelling.

A method for tracking both elliptical and rectangular extended objects using laser range sensors was presented in [3], and further studied for car tracking in [4]. The measurement pattern along the target contour was modelled by introducing so-called predicted measurements, which were used as the expectation for the measurements in a Gaussian mixture distribution. The Gaussian mixture PHD filter introduced in [5] was used for multi-target tracking in both [3] and [4]. The PHD filter was introduced in [6], and is based on the random finite set (RFS) formalism. A more recent RFS approach is the Poisson multi-Bernoulli mixture (PMBM) filter in [7] and [8], and stochastic optimization is used to handle the data association problem.

The probabilistic data association (PDA) filter presented in [9] is a popular method for tracking a single point target in clutter. The filter was later generalized to handle multiple target detections (MD-PDA) in [10], and further extended into a MD-JPDA filter in [11] to handle the multi-target tracking problem. Another generalization of the PDA was presented in [12] as the Generalized PDA (GPDA) for single-target tracking. In [13] the GPDA filter was used with the random matrix approach from [2] to track a boat with both radar and LIDAR.

The main contribution of this paper is to combine the EKF contour tracking approach from [3] with the GPDA data association scheme in order to develop a single-target tracking method suitable for boats of various sizes with LIDAR data. We compare it with the random matrix method in [13] through simulations and tracking a boat from real world data recorded at Trondheim Harbor, Norway. The modelling of the GPDA filter is slightly different from [12], and this will result in other association weights.

The paper is organized as follows: in section II we briefly present the state and measurement model and in section III we present the concept of GPDA. Section IV and V contains the results from simulations and real data, and section VI gives concluding remarks and suggestions for further work.

II. State and measurement modelling

The target state vector describes position, velocity and extent of the elliptical target at time step k, and is given by

$$\mathbf{x}_k = [x_k, y_k, v_{x,k}, v_{y,k}, a_k, b_k]^T, \quad k = 1, ..., T. \tag{1}$$

Here (x_k, y_k) is the ellipse center position, $(v_{x,k}, v_{y,k})$ is the velocities, and (a_k, b_k) are respectively the major and minor axes of the ellipse illustrated in Figure 1. We assume that the target evolves according to the linear dynamic model equation $\mathbf{x}_k = \mathbf{F}_{k-1}\mathbf{x}_{k-1} + \mathbf{q}_{k-1}$, where $\mathbf{q}_{k-1} \sim \mathcal{N}(\mathbf{q}_{k-1}; 0, \mathbf{Q}_{k-1})$ is the Gaussian process noise with covariance matrix $\mathbf{Q}_{k-1}$. The

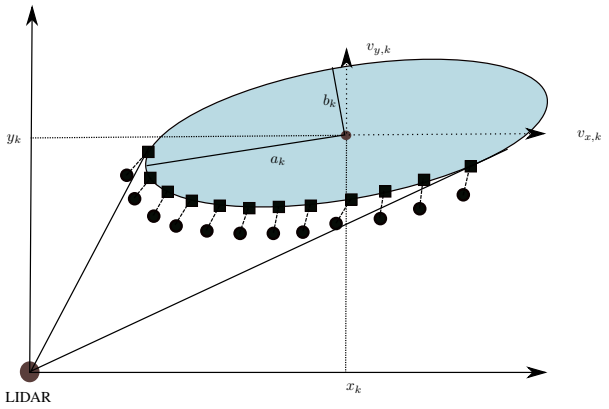

Fig. 1: Illustration of EOT with LIDAR. State variables, measurement generating points $\mathbf{y}_k^j$ (squares) along the target ellipse connected with associated measurements $\mathbf{z}_k^j$ (circles) are shown.

dynamic model matrix is given by

$$\mathbf{F}_{k-1} = \begin{bmatrix} 1 & 0 & \Delta t_k & 0 & 0 & 0 \\ 0 & 1 & 0 & \Delta t_k & 0 & 0 \\ 0 & 0 & 1 & 0 & 0 & 0 \\ 0 & 0 & 0 & 1 & 0 & 0 \\ 0 & 0 & 0 & 0 & 1 & 0 \\ 0 & 0 & 0 & 0 & 0 & 1 \end{bmatrix}. \tag{2}$$

The measurements for each time step k are given by the set $\mathbf{Z}_k = \{\mathbf{z}_k^j\}_{j=1}^{m_k}$ where the measurement vector consist of two-dimensional position coordinates given by $\mathbf{z}_k^j = [x_k^j, y_k^j]^T$ for all $j = 1, ..., m_k$. The cumulative measurement set $\mathbf{Z}_{1:k} = \{\mathbf{Z}_1, ..., \mathbf{Z}_k\}$ is defined to be a set of measurements for all time steps up to k. Each of the measurements in $\mathbf{Z}_k$ are assumed conditionally independent, and the likelihood can be expressed as

$$p(\mathbf{Z}_k|\mathbf{x}_k) = \prod_{j=1}^{m_k} p(\mathbf{z}_k^j|\mathbf{x}_k). \tag{3}$$

The LIDAR sensor sweeps the surveillance area and measures the bearing $\theta_k^j = \arctan2(y_k^j, x_k^j)$ and range $r_k^j = \sqrt{(x_k^j)^2 + (y_k^j)^2}$ for the closest object reflecting the laser beam. A target generated measurement $\mathbf{z}_k^j$ can be seen as a realization from a random measurement generating point $\mathbf{y}_k^j$ that is measured with some noise. The measurement generating points are given as nonlinear functions $\mathbf{y}_k^j(\cdot) : \mathbb{R}^{n_x} \to \mathbb{R}^{2m_k}$ of the target state vector. We assume that each measurement is generated by exactly one measurement generating point as shown in Figure 1. Now the measurement likelihood $p(\mathbf{z}_k^j|\mathbf{x}_k)$ for each measurement can be written as the convolution

$$p(\mathbf{z}_k^j|\mathbf{x}_k) = \int p(\mathbf{z}_k^j|\mathbf{y}_k^j(\mathbf{x}_k)) p(\mathbf{y}_k^j(\mathbf{x}_k)|\mathbf{x}_k) d\mathbf{y}_k^j(\mathbf{x}_k). \tag{4}$$

To find an analytical expression for this likelihood that corresponds with the distribution of real world data is challenging. However, we have assumed that each measurement comes from exactly one predicted measurement, and the density is simplified to

$$p(\mathbf{z}_k^j|\mathbf{x}_k) \approx \mathcal{N}\big(\mathbf{z}_k^j; \mathbf{y}_k^j(\mathbf{x}_k), \mathbf{R}_k^j\big), \tag{5}$$

where we have assumed a Gaussian likelihood for each measurement. The measurement generating points $\mathbf{y}_k^j(\mathbf{x}_k)$ are computed by using properties of the ellipse geometry, which is described in more detail in [3]. To calculate the covariance matrices $\mathbf{R}_k^j$ we use a diagonal noise matrix $\mathbf{R}_k = \text{diag}[\sigma_x^2, \sigma_y^2]$, and rotate it along the tangent line of the target ellipse. Hence it is given by $\mathbf{R}_k^j = \mathbf{R}_\phi(\phi_k^j)\mathbf{R}_k\mathbf{R}_\phi(\phi_k^j)^T$, where the angle ϕ_k^j is the rotation angle corresponding to the tangent line through $\mathbf{y}_k^j$, and $\mathbf{R}_\phi$ is the counterclockwise rotation matrix.

The likelihood of the measurements $\mathbf{Z}_k$, under the assumption that all are target originated, can now be expressed as

$$p(\mathbf{Z}_k|\mathbf{x}_k) \approx \prod_{j=1}^{m_k} \mathcal{N}(\mathbf{z}_k^j; \mathbf{y}_k^j(\mathbf{x}_k), \mathbf{R}_k^j). \tag{6}$$

III. Generalized Probabilistic Data Association

In this section we introduce clutter measurements. The measurement set is defined as $\mathbf{Z}_k = \Theta_k \cup K_k = \{\mathbf{z}_k^1, ..., \mathbf{z}_k^{m_k}\}$, where Θ_k and K_k are the sets of measurements from target and clutter, respectively. We define the number of target measurements as $|\Theta_k| = n_k^t$ and the number of clutter measurements as $|K_k| = n_k^c$, such that $m_k = n_k^t + n_k^c$.

The MD-PDA filter from [10] is based on the assumptions

- There is only one target of interest.
- The track has been initialized.
- The past information of the target is approximately summarized as

$$p(\mathbf{x}_k|\mathbf{Z}_{1:k-1}) \approx \mathcal{N}(\mathbf{x}_k; \mathbf{m}_{k|k-1}, \mathbf{P}_{k|k-1}). \tag{7}$$

- At each time step a validation region Γ_k is set up to validate each measurement.
- Among the validated measurements, one or more can originate from the target.
- The clutter measurements are modelled with uniform spatial distribution and Poisson cardinal distribution within the validation region.
- Target detections occur independently over time with known probability P_D.

These assumptions are similar to the traditional PDA, except for the number of points generated from target. In addition we assume that not more than n^{max} measurements are generated from target. This assumption is valid in the real data experiments, because we will use K-means clustering on the measurements, which gives $m_k = K$.

The validation region is an elliptical region where every measurement that is inside the region is included in the filtering step. We choose it to be a scaling of the predicted target state $\mathbf{m}_{k|k-1}$ in the extension variables with the validation region scale parameter γ_s. The volume of this validation region is

$$V_k = \pi\gamma_s^2 a_{k|k-1} b_{k|k-1}. \tag{8}$$

We define the set of mutually exclusive association hypotheses, when $m_k < n^{max}$, in the same way as in [12]

$$\mathcal{E} = \begin{cases} E^0 & = \{E_0^0 \quad \text{no detection from target} \\ E^1 & = \begin{cases} E_1^1 & \mathbf{z}_k^1 \text{ from target} \\ \vdots & \\ E_{m_k}^1 & \mathbf{z}_k^{m_k} \text{ from target} \end{cases} \\ E^2 & = \begin{cases} E_1^2 & \mathbf{z}_k^1,\, \mathbf{z}_k^2 \text{ from target} \\ E_2^2 & \mathbf{z}_k^1,\, \mathbf{z}_k^3 \text{ from target} \\ \vdots & \\ E_{\binom{m_k}{2}}^2 & \mathbf{z}_k^{m_k-1},\, \mathbf{z}_k^{m_k} \text{ from target} \end{cases} \\ & \vdots \\ E^{m_k} & = \{E_1^{m_k} \quad \text{all detections from target.} \end{cases}$$

The posterior pdf is defined according to the total probability theorem to be a weighted sum over all association hypotheses

$$p(\mathbf{x}_k|\mathbf{Z}_{1:k}) = \sum_{E_i^j \in \mathcal{E}} p(\mathbf{x}_k|E_i^j, \mathbf{Z}_{1:k}) P(E_i^j|\mathbf{Z}_{1:k}), \tag{9}$$

where the hypothesis conditional filtering density $p(\mathbf{x}_k|E_i^j, \mathbf{Z}_{1:k})$ needs to be computed for each hypothesis E_i^j. When not considering E_0^0, the index $j = 1, ..., m_k$ is the number of target generated points and $i = 1, ..., \binom{m_k}{j}$ is the hypothesis index within the hypothesis space E^j. If the target has a big extent and is within range of the LIDAR, it will most likely give at least one detection per time step, and we can write $P_D \approx 1$. In this paper we track a large passenger boat in a small harbor, and will assume that $P(E_0^0) \approx 0$. This assumption makes the GPDA derivation different from the approach in [12], where it is possible that the target does not exist or is not detected.

The association probabilities are denoted as the weights $\beta_k^{i,j}$ for each time step k, and can be written as

$$\beta_k^{i,j} = P(E_i^j|\mathbf{Z}_{1:k}) = P(E_i^j|\mathbf{Z}_k, m_k, \mathbf{Z}_{1:k-1}). \tag{10}$$

We prefer the last expression in (10) because it enables probabilistic inference on the number of measurements m_k.

Proposition 1. *Let the hypothesis conditional spatial densities be given as $p_{sp}(\Theta_k|E_i^j, m_k, \mathbf{Z}_{1:k-1})$ and $p_{sp}(K_k|E_i^j, m_k, \mathbf{Z}_{1:k-1})$ for the target and clutter measurements respectively, and let $P(n_k^t)$ and $P(n_k^c)$ be their corresponding prior cardinal densities. Then the association probability weights are given by*

$$\begin{aligned} \beta_k^{i,j} = &\frac{1}{C_\beta} p_{sp}(\Theta_k|E_i^j, m_k, \mathbf{Z}_{1:k-1}) \\ &\times p_{sp}(K_k|E_i^j, m_k, \mathbf{Z}_{1:k-1}) \binom{m_k}{j}^{-1} P(n_k^c) P(n_k^t), \end{aligned} \tag{11}$$

for $j = 1, ..., m_k$ and $i = 1, ..., \binom{m_k}{j}$, where C_β is the normalization constant.

Proof: We start by rewriting (10) using Bayes' formula

$$\beta_k^{i,j} = \frac{1}{C_\beta} p(\mathbf{Z}_k|E_i^j, m_k, \mathbf{Z}_{1:k-1}) P(E_i^j|m_k, \mathbf{Z}_{1:k-1}), \tag{12}$$

The association likelihood in (12) can be expressed by

$$\begin{aligned} &p(\mathbf{Z}_k|E_i^j, m_k, \mathbf{Z}_{1:k-1}) = \\ &\quad p_{sp}(\Theta_k|E_i^j, m_k, \mathbf{Z}_{1:k-1}) p_{sp}(K_k|E_i^j, m_k, \mathbf{Z}_{1:k-1}), \end{aligned} \tag{13}$$

where it is assumed that the target generated measurements are independent of the clutter measurements. Both the densities in (13) are spatial in the sense that we condition on m_k and E_i^j which leaves no uncertainty about the cardinalities n_k^t and n_k^c.

The predicted density in (11) is assumed independent of past measurements [12], i.e.

$$P(E_i^j|m_k, \mathbf{Z}_{1:k-1}) = P(E_i^j|m_k). \tag{14}$$

Then we observe that the joint density $P(E_i^j, n_k^t = j|m_k) = P(E_i^j|m_k)$ because the event E_i^j will be inside the event $n_k^t = j$. Using Bayes' rule, we then get

$$\begin{aligned} &P(E_i^j|m_k) = P(E_i^j, n_k^t = j|m_k) = \\ &\frac{P(E_i^j|n_k^t = j, m_k) P(m_k|n_k^t = j) P(n_k^t = j)}{P(m_k)} \\ &= \frac{1}{C_m} \binom{m_k}{j}^{-1} P(n_k^c = m_k - j) P(n_k^t = j). \end{aligned} \tag{15}$$

Here we have assumed that the density $P(E_i^j|n_k^t = j, m_k)$ is uniform over the hypothesis space E^j, which contains $\binom{m_k}{j}$ hypotheses. The density $P(m_k|n_k^t = j)$ is recognized as the clutter cardinal density $P(n_k^c = m_k - j)$ because of the relation $m_k = n_k^t + n_k^c$. Putting (13) together with (15) yields (11). ■

In the original formulation of the GPDA in [12], the cardinal densities $P(n_k^t|E_i^j, m_k, \mathbf{Z}_{1:k-1})$ and $P(n_k^c|E_i^j, m_k, \mathbf{Z}_{1:k-1})$ are modelled as a discrete uniform and Poisson respectively, which differs from our approach. We assume that n_k^t and n_k^c have prior densities given by

$$P(n_k^t) = \frac{1}{n^{max}}, \quad \text{for } n_k^t \geq 1 \tag{16}$$

$$P(n_k^c) = \frac{(\lambda V_k)^{m_k - j}}{(m_k - j)!} e^{-\lambda V_k}. \tag{17}$$

That is, the target generated points follow a discrete uniform distribution, while the number of clutter measurements are Poisson distributed with parameter λ. The value n^{max} is given by $n^{max} = m_k$, when m_k is known. We assume that $m_k < n^{max}$ in all experiments.

The clutter measurements have a spatial density over the validation region volume given by the uniform

$$p_{sp}(K_k|E_i^j, m_k, \mathbf{Z}_{1:k-1}) = (V_k)^{-(m_k - j)}. \tag{18}$$

By using Proposition 1 on the densities discussed so far, and excluding the constant terms, the association probabilities in (11) are

$$\beta_k^{i,j} \propto p_{sp}(\Theta_k|E_i^j, m_k, \mathbf{Z}_{1:k-1}) \frac{j!}{\lambda^j}. \tag{19}$$

These weights will prefer hypotheses with a high j because the factor $j!$ increases more rapidly than λ^j for $j = 1, ..., m_k$ and $\lambda < m_k$. This can happen if the spatial density term has the same magnitude as the prior term, but if $p_{sp}(\Theta_k|E_i^j, m_k, \mathbf{Z}_{1:k-1})$ is much higher it will be less significant.

The spatial density in (19) is given by the convolution

$$\begin{aligned} &p_{sp}(\Theta_k|E_i^j, m_k, \mathbf{Z}_{1:k-1}) = \\ &\int p(\tilde{\mathbf{z}}_k^{i,j}|E_i^j, m_k, \mathbf{Z}_{1:k-1}, \mathbf{x}_k) p(\mathbf{x}_k|E_i^j, m_k, \mathbf{Z}_{1:k-1}) d\mathbf{x}_k \\ &= \int \mathcal{N}(\tilde{\mathbf{z}}_k^{i,j}; \tilde{\mathbf{y}}_k^j(\mathbf{x}_k), \tilde{\mathbf{R}}_k^j) \mathcal{N}(\mathbf{x}_k; \mathbf{m}_{k|k-1}, \mathbf{P}_{k|k-1}) d\mathbf{x}_k, \end{aligned} \tag{20}$$

where $\tilde{\mathbf{z}}_k^{i,j} \in \mathbb{R}^{2j}$, $\tilde{\mathbf{y}}_k^j(\mathbf{x}_k) : \mathbb{R}^{n_x} \to \mathbb{R}^{2j}$ and $\tilde{\mathbf{R}}_k^j \in \mathbb{R}^{2j \times 2j}$ are the concatenated measurement vector for the target measurements $\mathbf{z}_k^{i,j} \in E_i^j$, and corresponding measurement model function and noise covariance matrix. To deal with the nonlinear measurement function $\tilde{\mathbf{y}}_k^j(\mathbf{x}_k)$ we use a first order Taylor expansion. The result of the integral in (20) then becomes

$$p(\Theta_k|E_i^j, m_k, \mathbf{Z}_k) = \mathcal{N}(\tilde{\mathbf{z}}_k^{i,j}; \tilde{\mathbf{y}}_k^j(\mathbf{m}_{k|k-1}), \mathbf{S}_{k|k-1}^j), \tag{21}$$

where the $2j \times 2j$ innovation covariance matrix is

$$\mathbf{S}_{k|k-1}^j = \mathbf{H}_k^j \mathbf{P}_{k|k-1} (\mathbf{H}_k^j)^T + \tilde{\mathbf{R}}_k^j. \tag{22}$$

The GPDA filter with random matrix is presented in [13], but we use Proposition 1 to define the association weights. In the experiments we use the traditional Kalman filter to compute the predicted mean $\mathbf{m}_{k|k-1}$ and covariance $\mathbf{P}_{k|k-1}$. The likelihood in (6) enables the use of extended Kalman filter (EKF), which computes the hypothesis conditional $p(\mathbf{x}_k|E_i^j, \mathbf{Z}_{1:k})$. To compute the filtered mean $\mathbf{m}_k$ and covariance $\mathbf{P}_k$, we do a moment-based mixture reduction akin to [9]. Since we do not have a closed form expression of the predicted measurement function, the Jacobian $\mathbf{H}_k^j$ is computed numerically using finite differences instead of being derived analytically. This method is referred to as the contour GPDA (C-GPDA).

IV. Simulation results

We simulate a target over $T = 200$ time steps with a time sampling interval of $\Delta t_k = 0.1$, which is also the true LIDAR sensor frequency used in the real data (Section V). The rest of the parameters are set as

$$\mathbf{R} = \text{diag}[0.1^2, 0.1^2], \quad \mathbf{x}_0 = [20, 20, 2, 2, 5, 1.5], \tag{23}$$

$$\mathbf{m}_0 = \mathbf{x}_0, \quad \mathbf{P}_0 = \mathbf{Q}, \quad \gamma_s = 4, \tag{24}$$

and the process noise covariance is

$$\mathbf{Q} = \begin{bmatrix} 10^{-5}/3 & 0 & 5 \cdot 10^{-5} & 0 & 0 & 0 \\ 0 & 10^{-5}/3 & 0 & 5 \cdot 10^{-5} & 0 & 0 \\ 5 \cdot 10^{-5} & 0 & 10^{-3} & 0 & 0 & 0 \\ 0 & 5 \cdot 10^{-5} & 0 & 10^{-3} & 0 & 0 \\ 0 & 0 & 0 & 0 & 10^{-4} & 0 \\ 0 & 0 & 0 & 0 & 0 & 10^{-4} \end{bmatrix}. \tag{25}$$

The target generates 10 measurements in each time step, and we distribute them along the visible target contour by using (5). The clutter points are from a Poisson distribution with parameter $\lambda = 2/V_\Lambda = 1/800$ and spatial window $\Lambda_k = [x_k - 20, x_k + 20] \times [y_k - 20, y_k + 20]$, with volume $V_\Lambda = 1600$. The filter assumes that the target generated points follow the uniform distribution from (16), but to narrow down the hypothesis space $\mathcal{E}$ we use an algorithm to bound the j-indices we want to investigate from below. This is done by removing outliers that are three scaled median absolute deviations (MADs) away from the rest of the validated measurements in x- or y-coordinates. Then we take the number of measurements that are left, and subtract it by the parameter g to find the lower bound n^{min} for j. In the simulation experiments we set $g = 3$.

We use the root-mean squared error (RMSE) to measure the absolute error of the filters. It is given by

$$\text{RMSE}_k^i = \sqrt{\frac{1}{N} \sum_{n=1}^{N} (\mathbf{m}_k^n[i] - \mathbf{x}_k^n[i])^2}, \tag{26}$$

where $i = 1, ..., n_x$. The notation $\mathbf{m}_k^n$ is the filtered value at time step k in the n-th Monte Carlo run, and $\mathbf{x}_k^n$ is the corresponding true state vector with size $n_x = 6$. In addition we use the normalized estimation error squared to measure the filter consistency. It is given by

$$\text{NEES}_k = \sum_{n=1}^{N} (\mathbf{m}_k^n - \mathbf{x}_k^n)^T (\mathbf{P}_k^n)^{-1} (\mathbf{m}_k^n - \mathbf{x}_k^n), \tag{27}$$

which is a $\chi^2_{n_x N}$-distributed variable. To measure the consistency we create a 95 % confidence interval and observe how many of the time steps the NEES is inside it. The formula for NEES in the random matrix estimates is given in [2].

The results from $N = 100$ Monte Carlo runs are summarized in Table I for both methods. We observe that the C-GPDA method has low absolute errors, while the random matrix estimates deviates more and are not consistent. This difference in estimation accuracy is probably caused by the measurement modelling of the two methods. The C-GPDA method is specifically designed for tracking with measurements along the target contour, while the random matrix method from [13] is a slightly modified version of the radar-based approach from [2]. The a_k-errors are a little bit higher than the b_k-errors because the target is initialized with only the rear end visible to the LIDAR. The NEES for C-GPDA lies inside the 95 % confidence interval for 95.41 % of the time, which means that it is covariance consistent with significance level 0.05. This type of NEES consistency analysis has not been done before when using the GPDA filter.

Observe that the lower bound algorithm is finding n^{min} to be below or equal to the true number of measurements from target in all time steps. This is important because it should not exclude the true association hypothesis when finding this lower bound.

Measure	C-GPDA	Random matrix GPDA
Mean x RMSE	0.0271	9.1145
Mean y RMSE	0.0256	3.3116
Mean v_x RMSE	0.0508	0.9654
Mean v_y RMSE	0.05	0.5965
Mean a RMSE	0.0358	0.8301
Mean b RMSE	0.0221	0.9717
Mean NEES	607.4672	36458, 1321
% confidence	0.9541	0.0051, 0
% where $n^{min} \leq 10$	100	100

TABLE I: Results from simulation experiments. The random matrix method has two entries in the NEES and confidence cell for kinematic and extent NEES defined in [2].

V. Real LIDAR data results

In this section we track a passenger boat departing from a pier in Trondheim, Norway. The LIDAR is placed on the pier which is the origin of the coordinate system. In Figure 2 the target vessel is depicted and from the picture we see that it is elliptically shaped in the front, but more rectangular in the rear end. The true length and width is 19.9 and 4.2 metres respectively, which gives the true major and minor axes as $a_k = 9.95$ and $b_k = 2.1$. We have no ground truth for the kinematical part of the target. The original LIDAR data set contains an average of 364 points per time step, and we need to reduce this number to narrow down the number of hypotheses. The K-means clustering algorithm is used with $K = 10$ because it maintains much of the original target information, while keeping $|\mathcal{E}|$ tractable in the GPDA algorithm. To initialize the target ellipse we used the least-squares ellipse fitting method from [14].

Fig. 2: Picture of the Munkholm boat MS Nidarholm in Ravnkloa, Trondheim.

The results of the C-GPDA tracking are shown in Figure 3. The lower bound n^{min} is found with $g = 1$ and the clutter intensity parameter is $\lambda = 1$. The results show that the C-GPDA method gives a reasonable estimate of the target position, heading and extent in all plotted time steps except for the last one, where only the rear end is visible to the LIDAR and it is difficult to get a good estimate of the full length. This can be seen in the RMSE for a_k in Figure 4a as well, and Figure 4b shows that the minor axis estimates is getting better because the LIDAR gives information about the width.

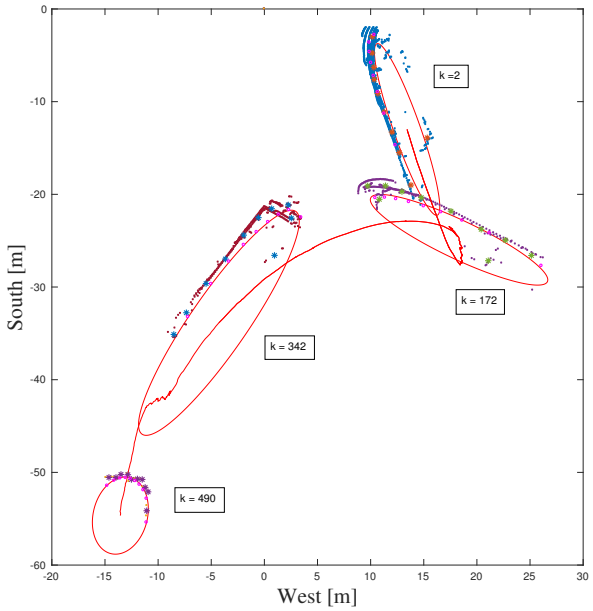

Fig. 3: Tracking plot of C-GPDA estimates $\mathbf{m}_k$ with target position and ellipse (red) together with the measurements and cluster centroids. Measurements and centroids are from $k = 2$ (blue, red), 172 (purple, beige), 342 (burgundy, blue), and 490 (purple). The predicted measurements $\mathbf{y}_k^j$ are plotted in magenta for all time steps.

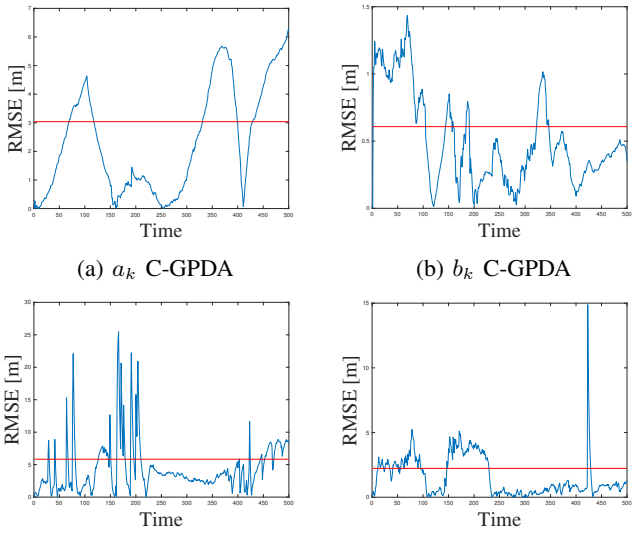

(a) a_k C-GPDA (b) b_k C-GPDA

(c) a_k random matrix (d) b_k random matrix

Fig. 4: RMSE plots for the extent estimates for a_k and b_k in the C-GPDA and random matrix GPDA methods on real LIDAR data. The red line is the mean RMSE.

In Figure 5 track results for the random matrix method with GPDA are shown. These are more deviant than the C-GPDA as we would expect from the simulation studies. The track is

irregular, and the extent estimate at $k = 172$ when the boat is turning is clearly wrong. From the extent RMSE plots in Figure 4c and 4d this can be seen as the peaks above the mean. In time steps $k = 250, ..., 400$ the extent estimates stabilizes more.

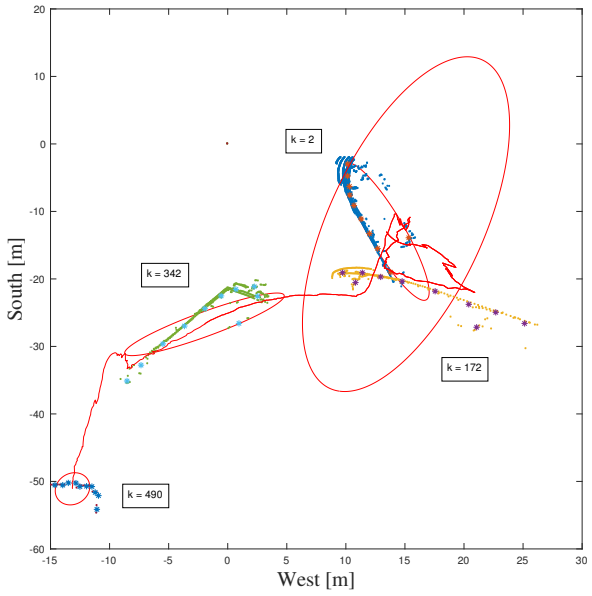

Fig. 5: Plot of random matrix estimated track and target ellipse on the cluster centroids. Measurements are from $k = 2$ (blue, red), 172 (beige, purple), 342 (green, cyan), and 490 (blue).

VI. Conclusion

In this paper we have combined the contour modelled EKF method with GPDA to track a single extended target in clutter using the LIDAR sensor. It has proven to be an accurate and consistent method in simulation experiments, and when tracking from real data. It outperforms the random matrix filter from [13] in all test cases. Further work could be to test the C-GPDA filter robustness to wake clutter akin to what was did for the PDA in [15]. It could also be compared against a point target tracking method using clustering on the measurements. To generalize C-GPDA into a multi-target method the framework of JPDA or the more general PMBM can be used.

Acknowledgment

This work was supported by the Research Council of Norway through projects 223254 (Centre for Autonomous Marine Operations and Systems at NTNU) and 244116/O70 (Sensor Fusion and Collision Avoidance for Autonomous Marine Vehicles). The authors would like to express great gratitude to Vegard Kamsvåg for recording the real-world lidar data. The work of the the second author is funded by DNV GL.

References

[1] J.W. Koch, "Bayesian approach to extended object and cluster tracking using random matrices", *IEEE transactions on aerospace and electronic systems*, vol. 44, no. 3, pp. 1042-1059, July 2008

[2] M. Feldmann, D. Fränken and J.W. Koch, "Tracking of extended objects and group targets using random matrices", *IEEE transactions on signal processing*, vol. 59, no. 4, pp. 1409-1420, April 2011.

[3] K. Granström, C. Lundquist and U. Orguner, "Tracking Rectangular and Elliptical Extended Targets Using Laser Measurements", *14th International Conference on Information Fusion*, Chicago, Illinois, USA, July 2011.

[4] K. Granström, S. Reuter, D. Meissner and A. Scheel, "A multiple model PHD approach to tracking of cars under an assumed rectangular shape", *17th International Conference on Information Fusion*, Salamanca, Spain, July 2014.

[5] K. Granström, C. Lundquist and U. Orguner, "Extended Target Tracking using a Gaussian-Mixture PHD filter", *IEEE transactions on aerospace and electronic systems*, vol. 48, no. 4, pp. 3268-3286, October 2012.

[6] R. Mahler, "Multitarget Bayes filtering via first-order multi target moments", *IEEE transactions on aerospace and electronic systems*, vol. 39, no. 4, pp. 1152-1178, October 2003.

[7] K. Granström, S. Reuter, M. Fatemi and L. Svensson, "Pedestrian tracking using velodyne data - Stochastic optimization for extended object tracking", *Proc. IEEE Intell. Veh. Symp.*, Redondo Beach, California, USA, pp. 39-46, July 2017.

[8] K. Granström, L. Svensson, S. Reuter, Y. Xia and M. Fatemi, "Likelihood-Based Data Association for Extended Object Tracking Using Sampling Methods", *IEEE Transactions on intelligent vehicles*, vol. 3, no. 1, pp. 30-45, December 2017.

[9] Y. Bar-Shalom and X.R. Li, *Multitarget-Multisensor Tracking*, YBS publishing, England, 1995.

[10] B. K. Habtemariam, R. Tharmarasa, T. Kirubarajan, D. Grimmett and C. Wakayama, "Multiple Detection Probabilistic Data Association filter for multistatic target tracking", *14th International Conference on Information Fusion*, Chicago, Illinois, USA, July 2011.

[11] B. K. Habtemariam, R. Tharmarasa, T. Thayaparan, M. Mallick, T. Kirubarajan, "A multiple-detection joint probabilistic data association filter", *IEEE. Sel. Topics Signal Process*, vol. 7, no. 3, pp. 461-471, June 2013.

[12] R. Schubert, C. Adam, E. Richter, S. Bauer, H. Lietz, and G. Wanielik, "Generalized Probabilistic Data Association for Vehicle Tracking under Clutter", *Intelligent Vehicles Symposium*, Alcal de Henares, Spain, pp. 962-968, July 2012.

[13] M. Schuster and J. Reuter, "Target Tracking in Marine Environment using Automotive Radar and Laser Range Sensor", *IEEE 20th International Conference on Methods and Models in Automation and Robotics*, Midzyzdroje, Poland, pp. 965-970, August 2015.

[14] A. Fitzgibbon, M. Pilu, and R. B. Fisher, "Direct Least Square Fitting of Ellipses", *IEEE Transactions on pattern analysis and machine intelligence*, vol. 21, no. 5, pp. 477-480, May 1999.

[15] E. Brekke, O. Hallingstad, and J. Glattetre, "Improved Target Tracking in the Presence of Wakes", *IEEE Transactions on Aerospace and Electronic Systems*, vol. 48, no. 2, April 2012.